

OPEN ACCESS

Periodic Modulations in an X-ray Flare from Sagittarius A*

To cite this article: G Bélanger *et al* 2006 *J. Phys.: Conf. Ser.* **54** 420

View the [article online](#) for updates and enhancements.

You may also like

- [The Impact of the Environment on the Early Stages of Radio Source Evolution](#)
Magosia Sobolewska, Aneta Siemiginowska, Matteo Guainazzi et al.
- [Developing the Physical Understanding of Intermediate Polars: An X-Ray Study of TV Col and V2731 Oph](#)
R. Lopes de Oliveira and K. Mukai
- [THE XMM-NEWTON AND INTEGRAL OBSERVATIONS OF THE SUPERGIANT FAST X-RAY TRANSIENT IGR J16328-4726](#)
M. Fiocchi, A. Bazzano, L. Natalucci et al.



ECS
The
Electrochemical
Society
Advancing solid state &
electrochemical science & technology

DISCOVER
how sustainability
intersects with
electrochemistry & solid
state science research

Periodic Modulations in an X-ray Flare from Sagittarius A*

G. Bélanger^{1,2}, R. Terrier², O.C. de Jager³, A. Goldwurm^{1,2}, F. Melia⁴

¹ Service d'Astrophysique, DAPNIA/DSM/CEA, 91191 Gif-sur-Yvette, France

² UMR Astroparticule et Cosmologie, 11 place Berthelot, 75005 Paris, France

³ Unit for Space Physics, North-West University, Potchefstroom 2520, South Africa

⁴ Physics Dept. and Steward Observatory, University of Arizona, Tucson, AZ 85721, USA

E-mail: belanger@cea.fr

Abstract. We present the highly significant detection of a quasi-periodic flux modulation with a period of 22.2 min seen in the X-ray data of the Sgr A* flare of 2004 August 31. This flaring event, which lasted a total of about three hours, was detected simultaneously by EPIC on *XMM-Newton* and the NICMOS near-infrared camera on the HST. Given the inherent difficulty in, and the lack of readily available methods for quantifying the probability of a periodic signal detected over only several cycles in a data set where red noise can be important, we developed a general method for quantifying the likelihood that such a modulation is indeed intrinsic to the source and does not arise from background fluctuations. We here describe this Monte Carlo based method, and discuss the results obtained by its application to other *XMM-Newton* data sets. Under the simplest hypothesis that we witnessed a transient event that evolved, peaked and decayed near the marginally stable orbit of the supermassive black hole, this result implies that for a mass of $3.5 \times 10^6 M_\odot$, the central object must have an angular momentum corresponding to a spin parameter of $a \approx 0.22$.

1. Introduction

Detecting Keplerian motion in the accretion flow orbiting around a black hole (BH), in the case where an event, localized to a portion of the flow, retains its coherence over several orbits, entails being able to detect periods of the order of 10^{-4} s (or frequencies of ~ 10 kHz) for solar mass objects. The problem is entirely different when considering a supermassive black hole (SMBH), and in particular Sgr A*. For a non-rotating BH of $3.5 \times 10^6 M_\odot$, the period at the marginally stable orbit (MSO, $r(\text{MSO}) = 3r_s = 6GM/c^2$) is 1592 s or about 26.5 min. So as much as detecting kHz quasi-periodic oscillations may be a delicate matter for certain reasons, as we explore long periodic signals, low frequency noise and windowing effects become important, and must be taken into account in a proper characterization of the signal.

In general, to test for a periodic signal, we must know what is the probability distribution function (PDF) of the test statistic in the absence of such a periodic signal, so that a reliable significance can be assigned to the claimed detection. In Fourier analysis, a PDF of the form e^{-Z} , where Z is the Fourier power gives the classical probability measure. For time series with important fluctuations or flares (colored noise), one usually obtains a distribution that is broader than e^{-Z} resulting in overestimated significances. Similarly, windowing effects introduced by

the testing of non-integral periods with respect to the total observation time also affect the probability distribution. These effects can be taken into account in order to derive an accurate probability for a given peak in the power spectrum.

For Sgr A*, the MSO—where we expect the minimum fundamental Keplerian period—ranges from $P_{\min} \sim 300$ to $P_{\max} \sim 1600$ s, for a mass of $3.5 \times 10^6 M_{\odot}$ and spin parameter $0 \leq a = \frac{Jc}{GM^2} < 0.999$. Here, J is the angular momentum, c is the speed of light, and G the gravitational constant. A number of X-ray observations of Sgr A* have revealed flares with durations between ≈ 3000 and 10000 s. We adopt a standard minimum quality factor, Q , of 4–5 cycles to claim a periodicity, and thus find that for the longest period of 1600 s, the minimum flare duration must be 8000 s. The number of Independent Fourier Spacings (IFS or trials) in our full interval (8752 s) is given by: $\text{IFS} = T_{\text{obs}}(1/P_{\min} - 1/P_{\max}) = 24$.

Aschenbach et al. (2004) claimed the detection of 5 periods ranging from 100 to 2250 s each of which were identified with one of the gravitational cyclic modes associated with accretion disks. The work of these authors was based on X-ray data from *XMM-Newton*. Genzel et al. (2003) claimed the detection of an ≈ 17 min period detected during two near-IR flares from Sgr A*. Clearly, a confirmed detection of a periodic or quasi-period signal present in a flare from the central BH would be very useful for constraining the nature of the flares, and more importantly, as evidence for the geometry of the space-time around Sgr A* through indirect BH spin measurements. In the context of this paper, we use the term *quasi-period* to refer to the average period of a signal that exhibits a periodic quality, while possibly comprising an evolution from longer to shorter periods, which would lead to a broader peak due to a spread in the power over several frequencies.

2. Observations and Methods

2.1. Observations

In the last few years, observations of the central BH with the *Chandra* and *XMM-Newton* X-ray telescopes have revealed several flares with different durations and spectral indices [2, 3, 11, 14]. Recently, two more flares were detected by *XMM-Newton*, and their properties are discussed by Bélanger et al. (2005).

Here, we restrict our analysis to *XMM-Newton* data, and pay particular attention to two data sets: 0516-0111350301 and 0866-0202670701. These observations of Sgr A* were respectively performed on 2002 October 3 and 2004 August 31, and each comprises one major flare, that lasted ~ 3 and 9 ks respectively. Details on the observation and characteristics of the first flare are presented and discussed by Porquet et al. (2003), and those of the other event by Bélanger et al. (2005). In addition, we analysed the data of pointing 0789-0202670601, which also comprised a flare from Sgr A*, but solar proton contamination caused a large number of data gaps during the flaring events thus making these data unreliable for period analysis. As described in Bélanger et al. (2005), the light curve can be reconstructed under the condition that the binning is large enough to be insensitive to the presence of very short good time intervals that would otherwise lead to an overestimate of the count rate. In this case, 500 s was found to be a reasonable bin size, but this does not allow a meaningful period analysis for an event that lasted ~ 3 ks.

For each data set, we used the PN event list constructed by selecting good X-ray events in the 2 – 10 keV energy range, within a radial distance of $10''$ from the radio position of Sgr A* [17]. The PN instrument has a larger collecting surface, better sensitivity and most importantly, a much higher time resolution than the MOS cameras— 73 ms compared to 2.6 s in *FullWindow* mode¹. This makes the PN camera the *XMM-Newton* instrument of choice for timing analysis. Figures 1 and 2 show the light curves of the 2004 August 31 flare and of the 2002 October 3 observations respectively, both with 120 s resolution.

¹ PN's time resolution can be as high as 0.3 ms in the standard *Timing* mode with a duty cycle close to 100%, and $7 \mu\text{s}$ in the special *Burst* mode. The duty cycle, however, is only 3% in the latter mode of operation.

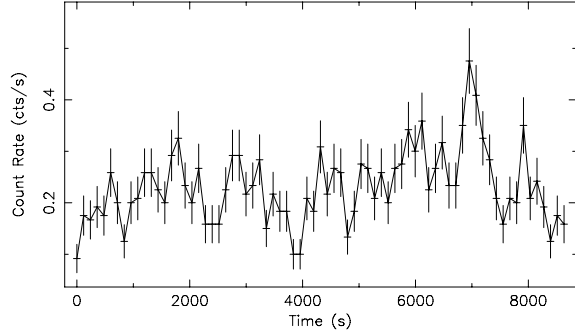


Figure 1. Light curve of the 2004 August 31 flare ($T \sim 9$ ks).

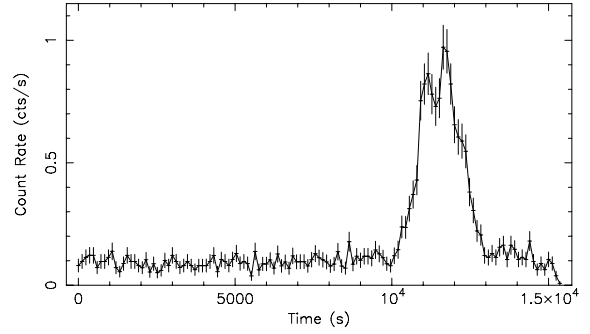


Figure 2. Light curve of complete ~ 15 ks 2002 October 3 observation.

2.2. Test-statistic and Periodogram

The Z^2 -periodogram is constructed as follows. For a given test period P_j , the phase ϕ_i , of each arrival time t_i , is calculated as $\phi_i = 2\pi t_i / P_j$. These phases are then used to calculate the Z_m^2 value defined by Buccheri et al. (1983) as

$$Z_m^2 = \frac{2}{N} \sum_{k=1}^m \left[\left(\sum_{i=1}^N \cos(k\phi_i) \right)^2 + \left(\sum_{i=1}^N \sin(k\phi_i) \right)^2 \right] \quad (1)$$

Here, N is the number of events and m is the number of harmonics over which the sum is performed. We used the Rayleigh statistic ($m=1$) and thus performed the sum over the first harmonic only, since this is the most powerful test for sinusoidal signals [12].

The Rayleigh statistic, Z_1^2 , is distributed as a χ^2 with two degrees of freedom (dof), or in compact form: $\chi_{\text{dof}}^2 = \chi_2^2$. This is so because $\cos \phi$ and $\sin \phi$ are Gaussian distributed, the square of a Gaussian variable is χ_1^2 distributed, and the sum of χ^2 variables is also a χ^2 variable for which the number of dof is given by the sum of the dof from the individual variables. Thus, the Z_m^2 statistic is χ_{2m}^2 distributed. de Jager (1994) showed that the predicted significance for a sinusoid from the Rayleigh power is

$$Y = -\log_{10}(\text{Prob}) = 0.434(Np^2/4 + 1), \quad (2)$$

where N is the number of events, and p is the pulsed fraction.

As mentioned above, the range of periods related to the MSO we consider physically interesting is 300–1600 s. Nonetheless, periodograms are shown from 100 s to $T_{\text{obs}}/3$.

2.3. Background

In the simplest case, the background is composed of white or Poisson noise: fluctuations for which the range of values is consistent with counting statistics. A more general case considers the background as a combination of white and red noise. Red noise (sometimes referred to as $1/f$ noise) arises from the inherent source variability and has a power spectral distribution that goes as $f^{-\alpha}$, where f is the frequency and α is the slope of the power spectrum in log-log space—the larger the amplitude of the variations, the steeper the slope.

Clearly, it is essential to determine the relative importance of the component of red noise with respect to the Poisson noise in order to accurately estimate the probability associated with a given peak in the periodogram. This can be done in different ways, one of which was recently suggested by Vaughan (2005) and entails determining the index α by performing a linear fit on the log-log periodogram and then calculating in an analytical way the confidence levels,

conveniently represented as lines parallel to, and lying above the fitted power-law. This method is simple, does not require Monte Carlo (MC) simulations, and is convenient for data that has an important component of red noise and whose duration is long enough to allow for a suitably large range of frequencies with a well defined power spectrum over which to perform the fit.²

Another way to characterize the component of red noise in an observation is to construct the power spectrum of the appropriately smoothed light curve. The power spectrum will then be dominated by the features associated with the inherent source variability, and will exhibit the features of the underlying red noise component, which can then be characterized as described above. This procedure should give results closely compatible with the method of de-trending—fitting the light curve with a polynomial and subtracting it—which leaves the flattened light curve free of the inherent source variability. Here, however, the stochastic nature of the red noise is not accounted for.

We have used a method that allows us to work directly with the event list and to take into account all noise components present in the data in a natural and transparent manner that also takes into account the random nature of the noise. This was done with the use of MC simulations to generate event lists having the same statistical properties as the data.

2.4. Pseudo-Random Event Lists

Most analyses aimed at estimating the significance of a periodic signal use MC simulations. We have used such a technique to estimate the probability of the null hypothesis, that is, the probability that a peak in the periodogram is caused by a background fluctuation. However, several different methods can be employed, and thus we detail the one we have used.

In counting photons from a given astrophysical source or radioactive decays from an unstable isotope, each event occurs independently of the previous but with a certain regularity given by the average count rate. These processes can be described by the same statistical law, characterised by an exponential PDF that defines the distribution of time intervals between two consecutive events and for which the mean corresponds to the average count rate. Therefore, in order to construct a true pseudo-random light curve of total duration T and average count rate r , one must draw $T \times r$ numbers from an exponential PDF with a mean of r . Each of these corresponds to the Δt between two consecutive events. Arrival times are calculated by summing these Δt , and the light curve is finally constructed from an event list that has the same statistical properties (Poissonian for $r = \text{const}$), as the data.

In the case where the mean is not constant, we can generate event lists with equivalent statistical properties as the data set by drawing the Δt s from different exponential PDFs with means determined by the sliding average count rate calculated from the data over an appropriately sized window.

The size of the smoothing window determines the range of periods accessible, (period longer than this size are smoothed out). By performing the simulations using different window sizes determined on the basis of the length of the observation as $T/4$, $T/8$, $T/16$, $T/32$, etc. down to a specified minimum, the probability associated with each trial period is determined taking into account fluctuations in the base level of the light curve that occur on timescales of the smoothing window size. Therefore, in each range of accessible trial periods, the significance of each peak is properly assessed. A period will be picked out only if it is significant compared to general trends in the light curve. Drawing numbers from PDFs with means that follow the variation in the count rate takes into account the overall noise properties of the data by simultaneously characterizing the inherent variations in the base level of the light curve, and allowing fluctuations about this level that are proportional to the amplitude of the variation. This is the method we used to estimate the probability associated with each value in the Rayleigh periodogram.

² A proper fitting technique must be used in order to determine the power-law index (see [10]).

In practice, for a given window size, we determine a set of mean rates and errors. For a mean rate $r \pm \sigma_r$, a Δt is constructed in two steps: one pseudo-random number, \hat{r} , is drawn from a Gaussian $N(r, \sigma_r)$, and another, $\Delta \hat{t}$, is drawn from an Exponential $E(\hat{r})$. The phases are constructed from the arrival times as described above. The full range of testable periods (chosen as $100-T/3$) is subdivided in 100 logarithmically spaced period bins, and logarithmically sampled by 150 trial periods, P_j , to ensure that each bin contains the same number of trials. For each P_j , we obtain a Z^2 value histogrammed in the corresponding period bin. Finally, the probability is determined directly from the Z^2 values by finding the quantile inverse for the Z^2 value of P_j in the data set.

3. Results

Figures 3 and 4 show the Z^2 -periodograms, and their associated probability as a function of period derived from the MC simulations for the flare data sets of 2004 August 31 and 2002 October 3 respectively. The In Fig. 5, we present the periodogram and probability of the data obtained on 2002 October 3 before the flare. The vertical scale is the same on all three Figures.

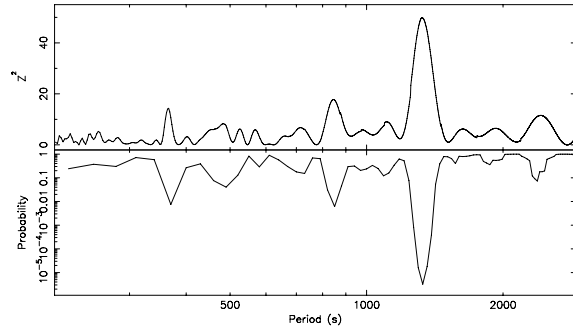


Figure 3. Flare of 2004 August 31: Z^2 -periodogram and associated probabilities derived from MC simulations of 10^6 event lists. Total flare duration was ~ 9000 s and thus the period range is 100–3000 s. The peak is at $P = 1330$ s and rises to a Z^2 value of 46, and has an associated probability of $\sim 10^{-6}$.

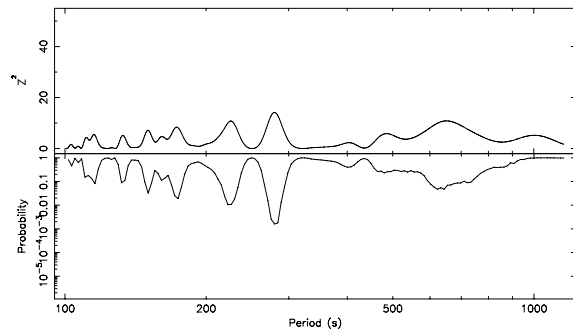


Figure 4. Flare of 2002 October 3: Z^2 -periodogram and associated probabilities derived from MC simulations of 500 event lists. Total flare duration is ~ 3000 s and period range spans 100–1000 s. No significant peaks are detected

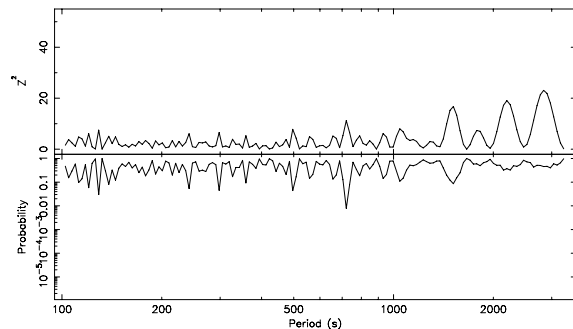


Figure 5. Data of 2002 October 3 before flare: Z^2 -periodogram and associated probabilities derived from MC simulations of 500 event lists. Total duration of observation is ~ 10000 s and period range spans 100–3000 s. No significant peaks are detected

As expected, the probability function is perfectly anticorrelated with the value of Z^2 over most of the range. Deviations are apparent towards to end of the range, where P_j becomes commensurable with T_{obs} . This effect is most noticeable in Fig. 5 where the last three peaks in the periodogram grow in height whereas their probabilities hover around one, indicating that the MC simulations indeed model the overall statistical properties of the data accurately and thus reproduce features associated with the noise. Notice that similar behaviour, although not as marked, is also seen in the 2004 August 31 as well as 2003 October 3 events.

In Fig. 3, the strongest peak at 1330 s has an associated probability of 3×10^{-6} . The other two noticeable peaks at 370 s and 850 s have respective probabilities of 0.006 and 0.007, and are therefore not significant. Peaks with probabilities greater than 10^{-3} cannot be considered significant if we apply a 3σ requirement to claim a detection and thus, no peaks in the periodograms other than the one at 1330 s can be taken as significant. The after-trial significance for this signal is $Y = 4.14$, and using Eq. 2 we find a pulsed fraction of 0.13 ($N = 2023$).

Fig. 6 presents three phasograms resulting from folding the flare light curve with a phase of 1330 s. These were constructed in the 2–4 keV, 4–10 keV and 2–10 keV bands. There is a clear asymmetry in the overall light curve, and a marked peak present at low energies, making the 2–4 keV band radically different from the much smoother 4–10 keV light curve. This peak is shifted by ~ 266 s from the centre of the sinusoid, corresponding to a distance of ~ 0.5 AU for light. This intriguing feature will be investigated elsewhere.

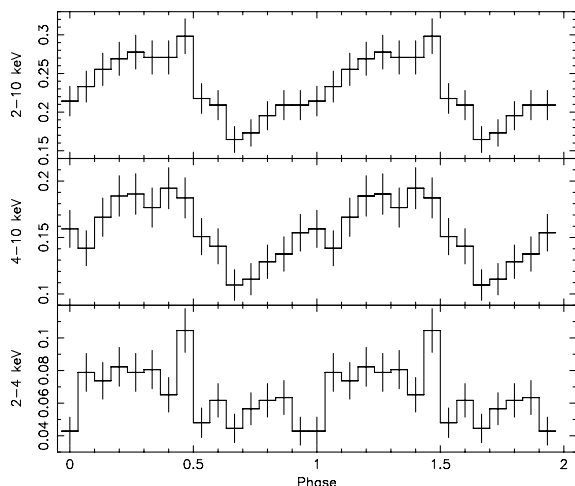


Figure 6. Light curve of 2004 August 31 flare folded with a phase of 1330 s, in three energy bands: 2–10 keV (top), 2–4 keV (middle) and 4–10 keV (bottom).

Finally, we also analyzed the pre-flare period of the 2002 October 3 observation to search for the periods reported by Aschenbach et al. (2004) in these data. The periodogram is shown in Fig. 5 and is remarkably flat over most of the range of physically interesting periods. As we can see from the associated probabilities, there are no significant peaks present.

4. Summary and Conclusion

We detected the presence of a 22.2 min quasi-period in the X-ray data of the flaring event in Sgr A* that occurred on 2004 August 31 while simultaneous *XMM-Newton* and HST observations were under way (see Yusef-Zadeh et al. 2006, Bélanger et al. 2005 and Bélanger et al. 2006 for details on the results of the campaign). The probability that such a signal arises from statistical fluctuations was determined to be 3×10^{-6} from MC simulations and is conservatively estimated to be less than $\sim 7.2 \times 10^{-5}$ if we consider the 24 IFS in the period range 300–1600 s [7]. It is important to clarify that although an evolution of the period as a function of time may be present (as expected from the spiraling motion), and that it can be qualitatively seen in the

light curve as alluded to by Liu et al. (2006), our statistics do not permit us to claim such a detection.

We considered and analysed two other *XMM-Newton* observations of Sgr A* using the same method for the probability estimation: the one that contains the 2004 March 31 flare, and the one of the 2002 October 3 flaring event. The former was found to be unreliable due to solar proton contamination, and no significant signals were detected in the latter, in contrast with the results obtained by Aschenbach et al. (2004) using the same data set.

The method we have developed to detect a periodic signal, and evaluate the associated probability is well suited for searches involving long periods with respect to the total observation time, and in which fluctuations in the average count rate do not follow Poisson statistics. This MC based method is just as powerful in the absence of red noise but clearly not necessary since the probability can be computed analytically. This straightforward and reliable method for quantitatively estimating the significance of a given periodic or semi-periodic modulation will be useful in future applications of this kind, and hopefully help, at least in part, relieve some of the ambiguities that arise in this type of analysis.

The radius of the MSO in units of $r_g = GM/c^2$ is given by:

$$r_{\text{mso}} = [3 + z_2 - \sqrt{(3 - z_1)(3 + z_1 + 2z_2)}], \quad (3)$$

where $z_1 = 1 + (1 - a^2)^{1/3}[(1 + a)^{1/3} + (1 - a)^{1/3}]$, and $z_2 = (3a^2 + z_1^2)^{1/2}$. The Keplerian frequency as a function of a is:

$$\omega = \frac{c^3}{2\pi GM} (r^{3/2} + a)^{-1}. \quad (4)$$

Taking a mass of $3.5 \times 10^6 M_\odot$ and assuming that the periodic signal originates from orbital motion at the MSO, the 1330 s period implies that the BH is spinning at a rate given by $a \approx 0.22$ (in the prograde case, the only considered).

Thus, the main result presented here can be interpreted as the signature of a transient event that evolved over about 10 ks, simultaneously giving rise to an X-ray and near-infrared flare. The emitting region spiraled around the mildly spinning SMBH, near or at the last stable orbit. In this simple scenario, we would have directly witnessed the accretion of matter through the accretion disk in the Kerr metric around the central dark mass (see [15]).

References

- [1] Aschenbach, B. et al. 2004, *A&A*, **417**, 71
- [2] Baganoff, F.K. et al. 2001, *Nature*, **413**, 45
- [3] Baganoff, F.K. et al. 2003, *ApJ*, **591**, 891
- [4] Bélanger, G. et al. 2005, *ApJ*, **635**, 1095
- [5] Bélanger, G. et al. 2006, *ApJ*, **636**, 275
- [6] Buccheri, R., et al. 1983, *A&A*, **128**, 245
- [7] de Jager, O.C., Swanepoel, J.W.H. & Raubenheimer, B.C. 1989, *A&A*, **221**, 180
- [8] de Jager, O.C. 1994, *ApJ*, **436**, 239
- [9] Genzel, R. et al. 2003, *Nature*, **425**, 934
- [10] Goldstein, M.L., Morris, S.A. & Yen, G.G. 2004, (cond-mat/0402322)
- [11] Goldwurm, A. et al. 2003a, *ApJ*, **584**, 751
- [12] Leahy, D.A., Elsner, R.F. & Weisskopf, M.C. 1983, *ApJ*, **272**, 256
- [13] Liu, S. Melia, F. & Petrosian, V. 2006, *ApJ*, **636**, 789
- [14] Porquet, D. et al. 2003a, *A&A*, **407**, L17
- [15] Tagger, M., & Melia, F. 2006, *ApJ*, **636**, L33
- [16] Vaughan, S. 2005, *A&A*, **431**, 391
- [17] Yusef-Zadeh, F., Choate, D., & Cotton, W. 1999, *ApJ*, **518**, L33
- [18] Yusef-Zadeh, F. et al. 2006, *ApJ*, **644**, 198